



Demianenko, M., Volf, M., Pavlenko, V., Liaposhchenko, O., Pavlenko, I. (2020). The solution of the stationary aeroelasticity problem for a separation channel with deformable sinusoidal walls. *Journal of Engineering Sciences*, Vol. 7(1), pp. D5–D10, doi: 10.21272/jes.2020.7(1).d2

The Solution of the Stationary Aeroelasticity Problem for a Separation Channel with Deformable Sinusoidal Walls

Demianenko M.¹*[0000-0002-4258-0379], Volf M.²[0000-0002-2904-8994], Pavlenko V.³,
Liaposhchenko O.¹[0000-0002-6657-7051], Pavlenko I.¹[0000-0002-6136-1040]

¹ Sumy State University, 2, Rymskogo-Korsakova St., 40007 Sumy, Ukraine;

² University of West Bohemia, 2738/8 Univerzitni St., 301 00 Pilsen 3, Czech Republic;

³ Machine-Building College of Sumy State University, 18, Shevchenka Ave., 40022 Sumy, Ukraine

Article info:

Paper received: January 22
The final version of the paper received: June 3, 2020
Paper accepted online: June 17, 2020

*Corresponding email:

m.demianenko@omdm.sumdu.edu.ua

Abstract. One of the most urgent problems concerning the design of inertial separation devices is the failure of the trapped liquid film from the contact surfaces due to the contact with the turbulent gas-liquid flow. For extension of the range of the effective inertial separation, a method of dynamic separation was proposed using the developed separation device with deformable sinusoidal walls. In this regard, the article is aimed at the development of the general methodology for the determination of the impact of hydrodynamic characteristics on the shape parameters for the deformed separation channel. The proposed approach is based on both physical and geometrical models. The first one allows obtaining compliance of deformable walls as a result of pressure distribution in the separation channel as a result of numerical simulation. The second one allows for obtaining variations of the main geometrical parameters of the proposed model using transfer functions. The relevancy of the proposed methodology was proved by the values of the relative errors for evaluating the variations of the amplitude and the radius of curvature.

Keywords: pressure field, elastic deformation, amplitude variation, elliptic integrals, transfer function, regression approach.

1 Introduction

At present, due to the specific energy consumption and separation efficiency, inertial and inertial-filtering separation approaches are widely used. However, one of the most common problems of their application is the failure of the trapped liquid film from the contact surfaces due to the contact with the turbulent gas-liquid flow. In this regard, the velocity and pressure fields are critical ones. An increase in the velocity of the gas-liquid flow leads to an increase in separation efficiency. After the velocity exceeds its critical value, the film of the trapped liquid breaks due to the appearance of waves on the interfacial surface and changes in the laminar mode to the turbulent one [1, 2].

There are following ways to solve the problem mentioned above [3]:

- 1) an increase in cross-section area for a decrease in gas velocity;
- 2) the use of nozzles with permanent drainage of a liquid;

3) reducing the mass ratio of a liquid and gas using pre-selection devices.

In this case, the critical velocity of the gas flow varies insignificantly. Therefore, there is still no significant extension in a range of effective operation of separation devices.

Due to the abovementioned, a method of dynamic separation is proposed. The corresponding separation equipment operates as an automatic control system, which is able to maintain the gas purification degree in a wide range of possible changes in the flow rate of the gas-liquid mixture. In this system, the object of regulation is hydraulic resistance, and the regulating impact is elastic forces. In this regard, the channel, which is bounded by sinusoidal walls, is proposed (Figure 1). These walls are fixed rigidly at the inlet of the gas-liquid flow. At the outlet, they have sliding fastening in the longitudinal direction.

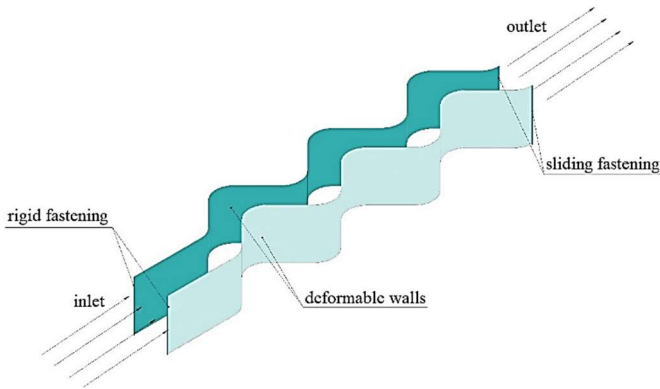


Figure 1 – The dynamic separation device with deformable sinusoidal walls

When the gas-liquid flow is passing through the separation channel, walls are changing their shape due to the hydrodynamic pressure. This affects the change of flow parameters and vice versa. Curved trajectories of liquid droplets, which are falling in the separation channel, are deviated from their initial ones. As a result, droplets are deposited on the walls with the formation of a liquid film. Finally, the deposited liquid flows out from the separation device through the drainage channels.

Since the gas-liquid flow changes in the shape of the separation channel, which in turn causes a change in flow parameters, the problem of aeroelasticity should be solved.

2 Literature Review

The scientific significance of the carried out research is highlighted by the absence of the corresponding experience of many authors in the field of designing of corresponding technological equipment. Particularly, an analysis of the steady flow of a viscous incompressible fluid in a channel with sinusoidal walls was presented by V. Borisov [4]. A perturbation method is developed in order to study viscous laminar flows through wavy-walled channels was applied by S. Tsangaris and L. Leiter [5]. The motion of particles in a viscous flow through a channel with sinusoidal walls was studied by E. Hasewaga and M. Saikai [6]. The system of differential equations of the particle movement, along with the sinusoidal surface, was solved by S. Pylypaka et al. [7].

Two-dimensional Stokes flow between sinusoidal walls was investigated by G. Bizatti, V. Di Federico, and S. Cintoli [8]. Two-dimensional steady fluid flow and heat transfer through a periodic wavy channel with staggered walls were numerically studied by H. Bahaidarah [9]. Additionally, the heat transfer and flow characteristics in corrugated sinusoidal wavy channels for the different phase shifts between the upper and lower wavy plates with the same equivalent diameter have been numerically investigated by J. Yin, G. Yang, and Y. Li [10].

Ways for modeling of fluid flow in two-dimensional sinusoidal corrugated channels were developed by A. Abdulsayid [11]. Analysis of fluid flow and heat transfer characteristics in sharp edge wavy channels was presented by M. Pervez, A. Aziz, and S. Chaturvedi [12].

Unsteady laminar flow of a Newtonian fluid in a channel with sinusoidal walls was numerically studied by Z. Mills et al. [13].

The effects of the wavy-wall phase shift on the thermal-hydraulic performance of fluid flow in the sinusoidal-wavy channel were studied by M. Ahmed et al. [14].

A methodology for static calculation of the dynamic deflection elements for separation devices was developed in [15]. Additionally, an approach for solving the stationary hydroaeroelasticity problem for dynamic deflection elements of separation devices was developed in [16]. This approach is valid for the automatic control system with dynamic separation elements. In this case, the regulation object is the hydraulic resistance.

An improvement of thermo-hydraulic performance, heat transfer, and pressure losses in a channel with the sinusoidal-wavy surface was provided by A. Boonloi and W. Jedsadaratanachai [17]. Finally, a parametric analysis of fluid flow through the heated corrugated channels was carried out by M. Salami, M. Khoshvaght-Aliabadi, and A. Feizabadi [18].

However, the approaches and methodologies mentioned above do not consider either deformation of walls or its automatic adjustment with the change in hydraulic losses during the operating process. Consequently, the presented research aims at the development of the general methodology for the determination of the impact of hydrodynamic characteristics on the shape parameters for the deformed separation channel.

3 Research Methodology

3.1 Mathematical modeling of wall's deformation

The development of the mathematical model of the wall's deformation is based on both the physical and geometrical approaches. For the case of linear material, the first one is based on the Hooke's law for isotropic material in compliance one-dimensional form [19] (Figure 2):

$$\Delta l = \delta \cdot F, \quad (1)$$

where Δl – displacement of the outer edge of the wall, m; δ – compliance, m/N.

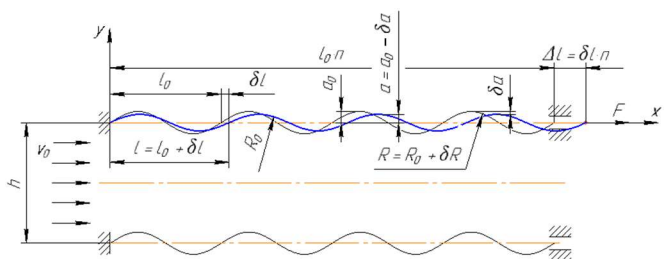


Figure 2 – The design scheme of a channel with deformable sinusoidal walls: h – average width, m; v_0 – inlet velocity, m/s; l_0 , l – lengths of a single wave, m; n – number of waves; a_0 , a – amplitudes, m; R_0 , R – radiuses of curvature, m; F – the equivalent force, N

The equivalent force F (N) can be determined numerically from the following energy condition:

$$A(F) = A(p), \quad (2)$$

where $A(F)$ and $A(p)$ – works of force F and hydrodynamic pressure p , respectively.

The geometrical model is based on the analysis of the change in parameters of the following sinusoidal curve (Figure 2):

$$y = a \cdot \sin \lambda x, \quad (3)$$

where x – longitudinal coordinate, m; a – amplitude, m; $\lambda = \frac{2\pi}{l}$ – the wave parameter (m^{-1}), which is inversely proportional to the length l , m.

The total length of a single wave is determined as follows:

$$L = \int_0^l \sqrt{1 + \left[\frac{dy(x)}{dx} \right]^2} dx. \quad (4)$$

The use of the incomplete elliptic Legendre integral of the second kind [20]:

$$E(k) = \int_0^{2\pi} \sqrt{1 - k^2 \sin^2 \theta} d\theta \quad (5)$$

allows rewriting the expression (4). In this case, after identical transformations, it should be written:

$$L = \frac{a}{k} E(k), \quad (6)$$

where $k = [0, 1)$ – the following dimensionless parameter:

$$k = \frac{a\lambda}{\sqrt{1+(a\lambda)^2}}. \quad (7)$$

It should be noted that in the case of relatively small amplitudes or large wavelengths, the dimensionless parameter can be simplified as $k \approx a \cdot \lambda$. Consequently, the total length of a single wave is determined as follows:

$$L = \frac{E(a\lambda)}{\lambda}. \quad (8)$$

The use of the small perturbation method allows writing the following:

$$L = L_0 + \delta L, \quad (9)$$

where $L_0 = E(a_0\lambda_0)/\lambda_0$ – the initial length (m), which depends on the initial values of the amplitude a_0 (m) and the wave parameter λ_0 (m^{-1}).

Due to the fact that the length is unchangeable during the deformation of a curved plate, the initial length L_0 retains constant ($L_0 = L = \text{const}$), and the infinitely small variation of the length is equal to zero. Consequently, the following equation can be written:

$$\delta L = - \left[\left(\frac{\partial L}{\partial a} \right)_0 \cdot \delta a + \left(\frac{\partial L}{\partial \lambda} \right)_0 \cdot \delta \lambda \right] = 0, \quad (10)$$

where δa – the variation of amplitude, m; $\delta \lambda$ – the variation of the wave parameter, m^{-1} :

$$\delta a = a_0 - a; \quad \delta \lambda = \lambda_0 - \lambda. \quad (11)$$

Equation (10) allows determining the variation of the amplitude:

$$\delta a = \Phi_0 \cdot \delta \lambda, \quad (12)$$

where $\Phi_0 = \Phi_0(a_0, \lambda_0)$ – the following transfer function:

$$\Phi_0(a_0, \lambda_0) = - \frac{\left(\frac{\partial L}{\partial \lambda} \right)_0}{\left(\frac{\partial L}{\partial a} \right)_0}. \quad (13)$$

3.2 Approximation of the developed model

Since the Legendre integral $E(k)$ is not integrable by quadratures, the following analytical expression is proposed for its approximation (Figure 3):

$$\tilde{E}(k) = \sqrt{4\pi^2 - \alpha^2 k^2}, \quad (14)$$

where α – the dimensionless parameter.

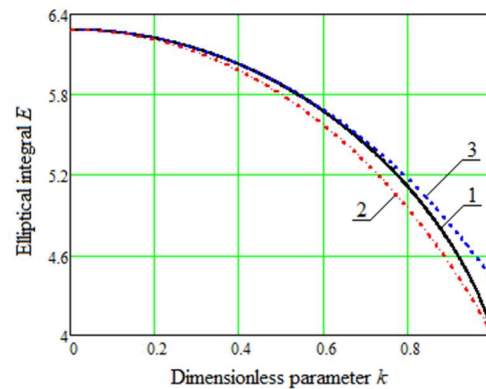


Figure 3 – Graphical representation of the elliptical integral (pos. 1) and its approximations (pos. 2, 3)

It should be noted that expression (14) should satisfy the following conditions: $\tilde{E}(0) = 2\pi$; $\tilde{E}(1) = 4$. The first condition is satisfied automatically, but the last one allows for obtaining the value $\alpha = (4\pi^2 - 16)^{1/2} \approx 4.85$. The corresponding approximating curve is marked in Figure 3 as pos. 2.

If the approximation accuracy is more valuable at the beginning part of the curve, the second condition is not accurately satisfied, and the parameter α mentioned above should be evaluated using the quasilinear regression approach [21]:

$$R = \sum_{i=1}^N [4\pi^2 - \alpha^2 k_i^2 - E^2(k_i)]^2 \rightarrow \min, \quad (15)$$

where R – the sum square error; i – index of experimental point; N – the total number of numerical experiments.

Minimization of the functional R with respect to the parameter α^2

$$\frac{\partial R}{\partial (\alpha^2)} = -2 \sum_{i=1}^N [4\pi^2 - \alpha^2 k_i^2 - E^2(k_i)] k_i^2 = 0 \quad (16)$$

allows determining the following regression dependence:

$$\alpha = \sqrt{\frac{\sum_{i=1}^N [4\pi^2 - E^2(k_i)] k_i^2}{\sum_{i=1}^N k_i^4}}. \quad (17)$$

In this case, after automatic tabulating values of $E(k_i)$ for a range of $k_i = [0, 1)$ using $N = 1 \cdot 10^4$ numerical experiments (with a constant step $1/N$), the following value of the evaluated parameter is obtained: $\alpha = 4.47$. The corresponding approximating curve is marked in Figure 3 as pos. 3.

In the case of using expression (14), the transfer function can be approximately determined as follows:

$$\Phi_0 \approx \frac{4\pi^2}{\alpha^2 a_0 \lambda_0^3}. \quad (18)$$

3.3 The radius of curvature

The radius of curvature of the sinusoidal curve in its amplitude values (Figure 2) as a parameter, which determines the losses along with the separation channel, is defined as follows:

$$R = \frac{\left\{1 + \left[\frac{dy(x)}{dx}\right]^2\right\}^{3/2}}{\left|\frac{d^2y(x)}{dx^2}\right|} = \frac{1}{a\lambda^2} = R_0 + \delta R, \quad (19)$$

where $R_0 = \frac{1}{a_0 \lambda_0^2}$ – the initial radius of curvature before deformations; δR – the variation of the radius of curvature, which is determined as follows:

$$\delta R = \left(\frac{\partial R}{\partial a}\right)_0 \cdot \delta a + \left(\frac{\partial R}{\partial \lambda}\right)_0 \cdot \delta \lambda. \quad (20)$$

The consequent consideration of expressions (20) and (18) allows obtaining the following variation from the last equation:

$$\delta R = \Psi_0 \delta \lambda, \quad (21)$$

where $\Psi_0 = \Psi_0(a_0, \lambda_0)$ – the following transfer function:

$$\Psi_0(a_0, \lambda_0) = \frac{2}{a_0 \lambda_0^3} \left[1 + \frac{2\pi^2}{(\alpha a_0 \lambda_0)^2}\right]. \quad (22)$$

Thus, the mathematical model is based on finding the transfer functions (13) and (22).

4 Results and Discussion

For numerical simulations of aeroelastic interaction of the gas flow with deformable sinusoidal walls, the “ANSYS Workbench” software with its modules “Fluent” and “Transient Structural” have been used. These modules are coupled by the module “System Coupling” and allow simulating hydrodynamics and studying elastic deformations of the system.

For modeling, the following physical parameters have been used: inlet velocity $v_0 = 15$ m/s; inlet and outlet hydraulic diameters are 0.12 m and 0.22 m, respectively; overpressure at the outlet 0 Pa; the turbulence model “k-ε”; the turbulence intensity 5%. The material properties are as follows: density 910 kg/m³; Young’s modulus $1.1 \cdot 10^6$ Pa; Poisson’s ratio 0.42. The initial geometrical parameters are as follows: width $h = 0.1$ m; length $l_0 = 0.312$ m; amplitude $a_0 = 0.052$ m.

The obtained numerical simulation results are presented in Figure 4.

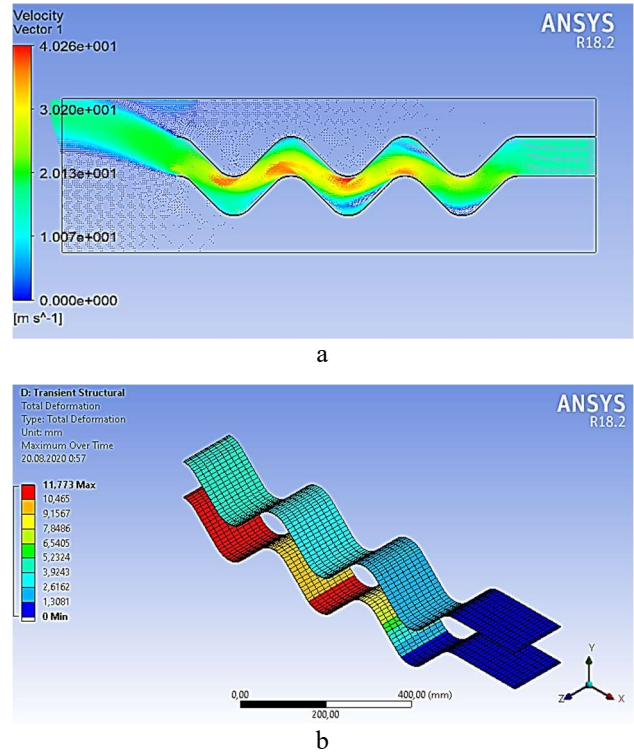


Figure 4 – The velocity field (a) and total deformations (b)

As a result of numerical simulation, the following parameters have been obtained: the equivalent force $F = 152$ N; the total longitudinal displacement $\Delta l = 4.6 \cdot 10^{-3}$ m.

The variation of the length for a single wave is equal to $\delta l = \Delta l/n = 4.6 \cdot 10^{-3}/3 = 0.0015$ (m). Compliance is equal to $\delta = \Delta l/F = 4.6 \cdot 10^{-3}/152 = 3.0 \cdot 10^{-5}$ (m/N).

The initial wave parameter $\lambda_0 = 20.138$ m⁻¹. The initial radius of curvature $R_0 = 0.0474$ m.

After deformations, the wave parameter $\lambda = 20.04$ m⁻¹. The initial radius of curvature $R = 0.0483$ m. Consequently, the corresponding variations are equal to $\delta \lambda = \lambda_0 - \lambda = 20.1 - 20.0 = 0.1$ (m⁻¹), and $\delta R = R - R_0 = 0.0005$ (m), respectively. Also, the amplitude $a = 0.0515$ m, and its variation $\delta a = a_0 - a = 5.17 \cdot 10^{-4}$ (m).

All the main parameters before and after deformations with the corresponding variations are summarized in Table 1.

Table 2 – The evaluated parameters of the mathematical model

Parameter	Initial value	Value after deformation	Variation
Displacement $\Delta l/n$, m	0.312	0.3135	0.0015
Wave parameter λ , m ⁻¹	20.138	20.040	0.098
Amplitude a , m	0.052	0.0515	0.0005
Radius of curvature R , m	0.051	0.0474	0.0009

It should be noted that the variation can be obtained from equation (13). In this case, the initial value of the transfer function is equal to $\Phi_0 = 5.2 \cdot 10^{-3}$ (m²), and the variation of the amplitude $\delta a = \Phi_0 \cdot \delta \lambda = 5.19 \cdot 10^{-4}$ (m).

Consequently, the relative error of evaluating the variation of the amplitude is equal to 1.2 %.

Finally, the variation of the radius of curvature can be obtained from equation (21). In this case, the initial value of the transfer function is equal to $\Psi_0 = 9.0 \cdot 10^{-3}$ (m²), and the variation of the radius of curvature $\delta R = \Psi_0 \cdot \delta \lambda = 8.82 \cdot 10^{-4}$ (m). Consequently, the relative error of evaluating the variation of the amplitude is equal to 7.0 %.

5 Conclusions

Thus, the stationary aeroelasticity problem for a separation channel with deformable sinusoidal walls has been solved. As a result, the general methodology for the determination of the impact of hydrodynamic characteristics on the shape parameters for the deformed separation channel has been developed. This methodology is based on both physical and geometrical approaches. The first one allows obtaining compliance of deformable walls as a result of pressure distribution in the separation channel. The second one is based on the analysis of the change in parameters of a sinusoidal curve.

As a result of numerical simulation for the inlet velocity of the gas flow 15 m/s, the equivalent force 152 N and the total longitudinal deformation $4.6 \cdot 10^{-3}$ m have been obtained. These data have allowed evaluating the compliance $3.0 \cdot 10^{-5}$ (m/N).

Additionally, according to the proposed methodology, variations of the main geometrical parameters of the

mathematical model have been calculated and summarized in Table 1.

The relevancy of the proposed approach using the transfer function is proved by the values 1.2 % and 7.0 % of the relative errors for evaluating variations of the amplitude and the radius of curvature, respectively.

Further research will be focused on studying the impact of the main parameters of the system “gas-liquid flow – deformable walls of the separation channel” to ensure the required separation efficiency, as well as on the identification of non-stationary hydrodynamic effects in this system.

6 Acknowledgments

The developed methodology was realized within the research projects “Development and Implementation of Energy Efficient Modular Separation Devices for Oil and Gas Purification Equipment” (State reg. No. 0117U003931), and “Creation of new granular materials for nuclear fuel and catalysts in the active hydrodynamic environment” (State reg. No. 0120U102036) ordered by the Ministry of Education and Science of Ukraine.

Computer means for numerical simulations were realized within the internship “CFD simulation of the heat and mass transfer processes between liquid and gas phases of the mixture flow inside of the chemical equipment” at the University of West Bohemia.

References

1. Gokhale, S. J., Plawsky, J. L., Wayner, P. C. (2004). Inferred pressure gradient and fluid flow in a condensing sessile droplet based on the measured thickness profile. *Physics of Fluids*, Vol. 16(6), pp. 1942–1955, doi: 10.1063/1.1718991.
2. Chernyshenko, S. I., Goulart, P., Huang, D., Papachristodoulou, A. (2014). Polynomial sum of squares in fluid dynamics: A review with a look ahead. *Philosophical Transactions of the Royal Society A: Mathematical, Physical and Engineering Sciences*, Vol. 372, 20130350, doi: 10.1098/rsta.2013.0350.
3. Lioumbas, J. S., Paras, S. V., Karabelas, A. J. (2005). Co-current stratified gas-liquid downflow – Influence of the liquid flow field on interfacial structure. *International Journal of Multiphase Flow*, Vol. 31(8), pp. 869–896, doi: 10.1016/j.ijmultiphaseflow.2005.05.002.
4. Borisov, V. I. (1982). Viscous liquid flow in a channel with sinusoidal walls. *Journal of Engineering Physics*, Vol. 42, pp. 399–401, doi: 10.1007/BF00826839.
5. Tsangaris, S., Leiter, E. (1984). On laminar steady flow in sinusoidal channels. *Journal of Engineering Mathematics*, Vol. 18, pp. 89–103, doi: 10.1007/BF00042729.
6. Hasewaga, E., Saikai, M. (1988). On the trajectories of a small particle passing through a narrow curved channel. *Transactions of the Japan Society of Mechanical Engineers, Part B*, Vol. 54(507), pp. 3061–3068, doi: 10.1299/kikaib.54.3061.
7. Pylypaka, S., Volina, T., Mukvich, M., Efremova, G., Kozlova, O. (2020). Gravitational relief with spiral gutters, formed by the screw movement of the sinusoid. *Advances in Design, Simulation and Manufacturing III. DSMIE 2020. Lecture Notes in Mechanical Engineering*, pp. 63–73, doi: 10.1007/978-3-030-50491-5_7.
8. Bizzarri, G., Di Federico, V., Cintoli, L. S. (2002). Stokes flow between sinusoidal walls. *Advances in Fluid Mechanics IV*, pp. 323–332.
9. Bahaidarah, H. M. S. (2007). A numerical study of fluid flow and heat transfer characteristics in channels with staggered wavy walls. *Numerical Heat Transfer, Part A: Applications*, Vol. 51(9), pp. 877–898, doi: 10.1080/10407780600939644.
10. Yin, J., Yang, G., Li, Y. (2012). The effects of wavy plate phase shift on flow and heat transfer characteristics in corrugated channel. *Energy Procedia*, Vol. 14, pp. 1566–1573, doi: 10.1016/j.egypro.2011.12.1134.
11. Abdulsayid, A. G. A. (2012). Modeling of fluid flow in 2D triangular, sinusoidal, and square corrugated channels. *International Journal of Chemical and Molecular Engineering*, Vol. 6(11), doi: 10.5281/zenodo.1333624.

12. Pervez, M., Aziz, A., Chaturvedi, S. (2013). Analysis of fluid flow and heat transfer characteristics in sharp edge wavy channels with horizontal pitch on both edges. *International Journal of Engineering Research and Technology*, Vol. 2(6), pp. 162–180.
13. Mills, Z. G., Shah, T., Warey, A., Balestrino, S., Alexeev, A. (2014). Onset of unsteady flow in wavy walled channels at low Reynolds number. *Physics of Fluids*, Vol. 26, 084104, doi: 10.1063/1.4892345.
14. Ahmed, M. A., Yusoff, M. Z., Ng, K. C., Shuai, N. H. (2014). The effects of wavy-wall phase shift on thermal-hydraulic performance of Al₂O₃–water nanofluid flow in sinusoidal-wavy channel. *Case Studies in Thermal Engineering*, Vol. 4, pp. 153–165, doi: 10.1016/j.csite.2014.09.005.
15. Pavlenko, I. V., Liaposhchenko, O. O., Demianenko, M. M., Starynskyi, O. Ye. (2017). Static calculation of the dynamic deflection elements for separation devices. *Journal of Engineering Sciences*, Vol. 4(2), pp. B19–B24, doi: 10.21272/jes.2017.4(2).b19.
16. Pavlenko, I., Liaposhchenko, O., Ochowiak, M., Demyanenko, M. (2018). Solving the stationary hydroaeroelasticity problem for dynamic deflection elements of separation devices. *Vibrations in Physical Systems*, Vol. 29, 2018026.
17. Boonloi, A., Jedsadaratanachai, W. (2019). Thermo-hydraulic performance improvement, heat transfer, and pressure loss in a channel with sinusoidal-wavy surface. *Advances in Mechanical Engineering*, Vol. 11(9), pp. 1–17, doi: 10.1177/1687814019872573.
18. Salami, M., Khoshvaght-Aliabadi, M., Feizabadi, A. (2019). Investigation of corrugated channel performance with different wave shapes. *Journal of Thermal Analysis and Calorimetry*, Vol. 138, pp. 3159–3174, doi: 10.1007/s10973-019-08361-y.
19. Zheng, Q. (2002). Constitutive relations of linear elastic materials under various internal constraints. *Acta Mechanica*, Vol. 158(1-2), pp. 97–103, doi: 10.1007/BF01463172.
20. Wang, F., Guo, B., Qi, F. (2020). Monotonicity and inequalities related to complete elliptic integrals of the second kind. *AIMS Mathematics*, Vol. 5(3), pp. 2732–2742, doi: 10.3934/math.2020176.
21. Pavlenko, I., Trojanowska, J., Ivanov, V., Liaposhchenko, O. (2019). Parameter identification of hydro-mechanical processes using artificial intelligence systems. *International Journal of Mechatronics and Applied Mechanics*, Vol. 2019(5), pp. 19–26.